2840 *Macromolecules* **2010**, *43*, 2840–2845
DOI: 10.1021/ma902789g

Macromolecules
ARTICLE

Molecular Hybrid Optical Limiting Materials from Polyhedral Oligomer Silsequioxane: Preparation and Relationship between Molecular Structure and Properties

Xinyan Su,[†] Shanyi Guang,[†] Changwei Li,[‡] Hongyao Xu,*[,†,§] Xiangyang Liu,[⊥] Xin Wang,[†] and Yinglin Song[‡]

[†]*College of Material Science and Engineering & State Key Laboratory for Modification of Chemical Fibers and Polymer Materials, Donghua University, Shanghai 201620, China,* [‡]*Department of Physics, Suzhou University, Suzhou 215008, China,* [§]*State Key laboratory of Crystal Materials, Shandong University, Jinan 250100, China, and* [⊥]*Department of Physics, National University of Singapore, 117542 Singapore*

Received December 17, 2009; Revised Manuscript Received February 10, 2010

ABSTRACT: A series of new molecular hybrids with stilbene chromophore (**H1**−**H4**) are prepared by hydrosilylation of octahydridosilsesquioxane ($\mathbf{T_8^H}$). All these stilbene-containing hybrid materials are soluble in common organic solvents, such as chloroform, toluene, THF, and 1,2-dichloroethane, and possess good film-forming properties. Their structures and properties are characterized and evaluated by FT-IR, NMR, UV, PL, TGA, DSC, nonlinear optical (NLO), and optical limiting (OL) analyses. The results show that the thermal decomposition temperatures (T_d, 5 mass % loss) of the hybrids are 20−60 °C greater than their corresponding stilbene monomers, and the hybrids show obvious nonlinear absorption (β up to 2.56×10^{-11} m/W) and optical limiting properties. The larger excited-state absorption cross sections than corresponding ground-state absorption cross sections of the hybrids indicate that reverse saturable absorption is a major mechanism responsible for the optical limiting of the hybrids.

Introduction

π-Conjugated organic nonlinear optical (NLO) materials are promising OL materials owing to their fast response time, high damage threshold, and ease of structure modification.[1−5] However, their poor processability and low thermal stability have limited their application in optical limiting devices. Organic−inorganic nanocomposites are of great interest because they offer the potential to realize remarkable and complementary properties that cannot be obtained from a single material. However, inhomogeneity of the dispersion of inorganic particles in composites often results in low transmittance and has limited their application in optical devices.[6] Molecular hybrids, which contain an inorganic phase bonded (often covalently) to an organic phase, can effectively solve the problem of uniform dispersion of inorganic particles in composites and have attracted great interest.[7−9] Nevertheless, the major challenge is how to bind an organic compound covalently with inorganic moieties during synthesis.

Polyhedral oligomeric silsesquoixanes (POSS) are a class of inorganic compounds with nanoscale dimensions (0.5−3 nm) with well-defined cubeoctameric structures with a silica-like core (Si_8O_{12}) surrounded by eight organic corner groups (functional or inert),[10,11] which makes POSS molecules excellent platforms and blocks for nanotechnology applications and for assembly of novel organic/inorganic hybrid nanocomposites. More importantly, new hybrids with POSS incorporated at the molecular level can overcome the aggregation effect which often occurs in common hybrid composites based on a physical mixture. Thus, POSS molecules with unique structure provide the best homogeneity, reproducibility, predictability of hybrids, and the opportunity to tailor materials' properties. Many POSS-based hybrid nanocomposites with different architectures (linear or pendant,[9,12−16] star,[8,17−19] and network structures[20,21]) have been prepared, and their thermal properties and the reason for enhanced thermal properties were investigated. Recently, researchers are shifting their interests toward functional molecular hybrids with novel functional properties such as low dielectric constant,[20,22] good luminescence performance,[23−28] high rigidity,[29] resist coatings for lithography,[30] and so on. To the best of our knowledge, however, the hybrids with nonlinear optical and optical limiting properties have rarely been reported.[31,32]

Recently, we reported the design and controllable preparation of a series of novel soluble optical limiting functional hybrids with different architectures such as dumbbell, bead, or network-type structures, based on the hydrosilylation reactions of octahydridosilsesquioxane and different azobenzene chromophore monomers.[7] To further explore the influence of the molecular structure on optical limiting properties, in this paper, a series of star-type POSS-based molecular hybrid optical limiting materials were prepared (Scheme 1), and the relationship between molecular structure and their optical properties and the possible mechanism responsible for the optical limiting of hybrids were investigated.

Experimental Section

Materials. Octahydridosilsesquioxane [$(HSiO_{1.5})_8$, $\mathbf{T_8^H}$] was synthesized according to the procedures described in ref 33. The synthesis and characterization of the monomers 1-butoxy-4-(4-ethynylstyryl)benzene (**M1**), 1-(decyloxy)-4-(4-ethynylstyryl)-benzene (**M2**), 1-ethynyl-4-(4-(hexadecyloxy)styryl)benzene (**M3**), and 1-ethynyl-4-(4-nitrostyryl)benzene (**M4**) are described elsewhere.[3] All the chromophores link with a terminal alkynyl bond as the reactive group. **H1**−**H4** were prepared by hydrosilylation between **M1**−**M4** and multifunctional $\mathbf{T_8^H}$, as shown

*Corresponding author: Tel +86-21-67792874, e-mail hongyaoxu@163.com.

 Published on Web 02/23/2010

Scheme 1. Synthesis Method for Preparation of POSS-Based Hybrids H1−H4

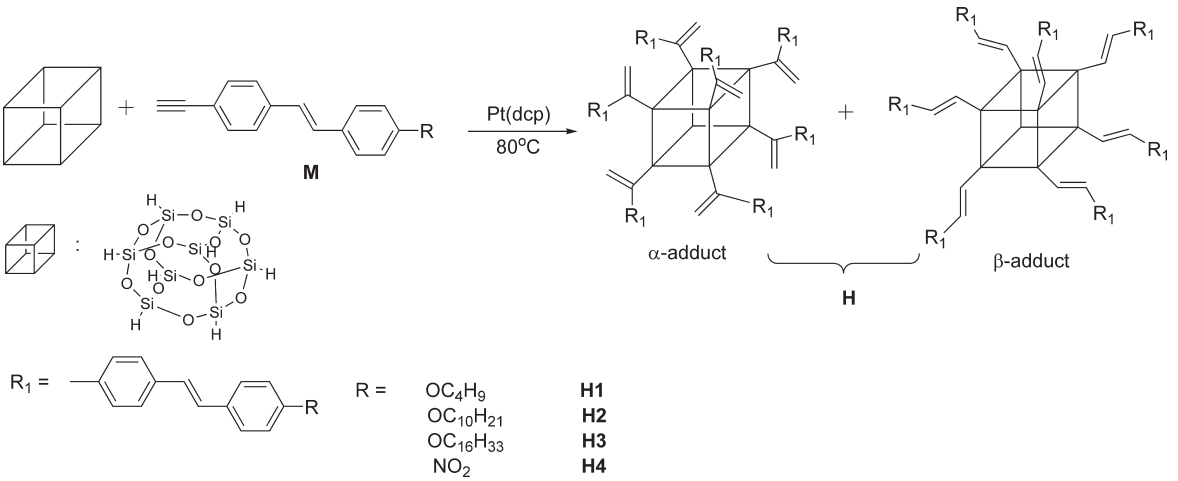

in Scheme 1. The platinum dicyclopentadiene complex, [Pt(dcp)], was synthesized by the following literature procedures[34] and used as a 2 mM solution in $C_2H_4Cl_2$.

Synthesis of the Molecular Hybrids. The hydrosilylation reaction for preparing starlike hybrid was carried out under nitrogen using a vacuum-line system. A typical reaction is shown as the general reaction: 5 mL of $C_2H_4Cl_2$, 21.2 mg (0.05 mmol) of octahydridosilsesquioxane ($\mathbf{T_8^H}$), 1.0 mg of Pt(dcp), and 0.11 g (0.40 mmol) of 1-butoxy-4-(4-ethynylstyryl)benzene (**M1**) were added into 20 mL Schlenk tube with a side arm. The reaction mixture was stirred at 80 °C for 10 h. The mixture was then poured into excess hexane, with vigorous agitation to dissolve the unreacted POSS and precipitate the desired hybrid. The precipitate was centrifuged and redissolved in minimal THF (ca. 3 mL). Then the THF solution was added dropwise into 200 mL of hexane to precipitate the product. The dissolution−precipitation process was repeated three times, and the finally isolated precipitant was dried in vacuum at 80 °C to a constant weight and to get a pale powder (**H1**).

Instruments. FTIR spectra of KBr disks were measured with a Nicolet NEXUS 870 FTIR spectrophotometer at room temperature; 32 scans were collected at a resolution of 1 cm^{-1}. ^1H NMR (300 MHz), ^{13}C NMR (100 MHz), and ^{29}Si NMR (79.49 MHz) spectra were recorded on a Bruker DMX-400 spectrometer utilizing tetramethylsilane (TMS, 0.00 ppm) as the internal standard in chloroform-*d* ($CDCl_3$) at room temperature. Weight-average (M_w) and number-average (M_n) molecular weights and polydispersity index (PDI, M_w/M_n) were determined by a gel permeation chromatograph (GPC) using a Waters 510 HPLC equipped with a Rheodyne 7725i injector with a stand kit, a set of Styragel columns (HT3, HT4, and HT6; molecular weight range 10^2-10^7), a column temperature controller, a Waters 486 wavelength-tunable UV−vis detector, a Waters 410 differential refractometer, and a system DMM/scanner possessing an eight-channel scanner option. All hybrid solutions were prepared in THF (ca. 2 mg/mL) and filtered through 0.45 μm PTFE syringe-type filters before injected into the GPC system. THF was used as the eluent at a flow rate of 1.0 mL/min. The column temperature was maintained at 30 °C, and the working wavelength of the UV detector was set at 254 nm. A set of monodisperse polystyrene standards (Waters) was used for calibration purposes. Differential scanning calorimetry (DSC) was performed on a TA Instruments DSC 9000 equipped with a liquid nitrogen cooling accessory (LNCA) unit under a continuous nitrogen purge (50 mL/min). The scan rate was 10 °C/min within the temperature range 30−250 °C. Samples (4−6 mg) were weighed and sealed in aluminum pans. Thermogravimetric analysis (TGA) was carried out using a TA Instruments TGA 2050 thermogravimetric analyzer with a heating rate of 10 °C/min from 30 to 700 °C under a continuous nitrogen purge (100 mL/min). Samples (15−25 mg) were loaded in alumina pans. The thermal degradation temperature (T_d) was defined as the temperature of 5% mass loss. UV spectra of the hybrids were investigated in THF (ca. 2×10^{-6} M) at room temperature in 1 cm quartz cell using a Shimadzu UV-265 spectrometer.

The nonlinear absorption properties of the samples were performed by open *Z*-scan technique with a frequency doubled, Q-switched, mode-locked Continuum ns/ps Nd:YAG laser system, which provides linearly polarized 4 ns optical pulses at 532 nm wavelength with a repetition of 1 Hz. The experiment was set up as in the literature.[35] The spatial distribution of the pulse is nearly a Gaussian profile. The THF solution of the hybrid (concentration: $c = 0.005$ M) was contained in a quartz cell with the thickness of 2 mm. The samples were placed on a translation stage controlled by a computer and moved along the *z*-axis with respect to the focal point of a 300 mm focal len. The input energy was 62 μJ. The radius ω_0 at beam waist was 50 mm. The input laser pulses adjusted by an attenuator (Newport) were split into two beams. The two beams were simultaneously measured by using two energy detectors, D1 and D2 (Rjp-735 energy probes, Laser Precision).

The investigation of the optical limiting properties of the samples was carried out by using the same laser system as in the nonlinear absorption experiment. The experimental arrangement is similar to that in the literature.[36] The samples were housed in quartz cells with a thickness of 2 mm and positioned at the focal point.

Results and Discussion

Synthesis. It is reported that substituted stilbenes are well-known π-conjugated NLO chromophores and possess good optical limiting properties under high transmittance.[37] However, the inherent drawbacks of small molecules, such as poor processability and low thermal stability, often limited their application. POSS core not only provides the heat capacity of silica but also acts as electron acceptor.[38] Therefore, introduction of POSS into stilbene chromophores will be expected to combine the advantages of both POSS and stilbenes. Simultaneously, the terminal flexible alkoxyl-substituted groups were incorporated into the stilbene to improve the solubility and film-forming properties of the resultant hybrids and explore the influence of molecular structure on their optical properties.[39] These resultant **H1−H4** hybrids were prepared by hydrosilylation between organic stilbene chromophore monomers **M1−M4** and $\mathbf{T_8^H}$

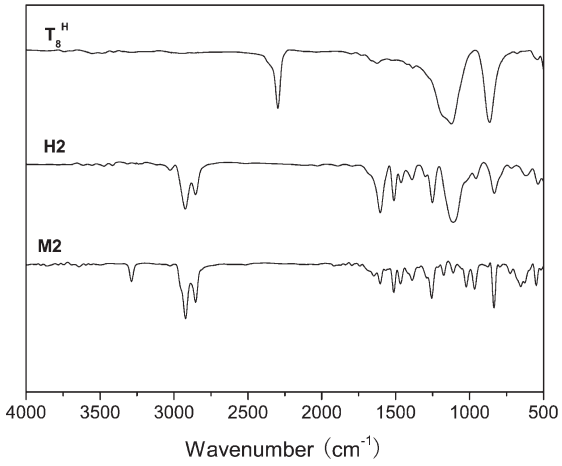

Figure 1. IR spectra of $\mathbf{T_8^H}$, **M2**, and **H2**.

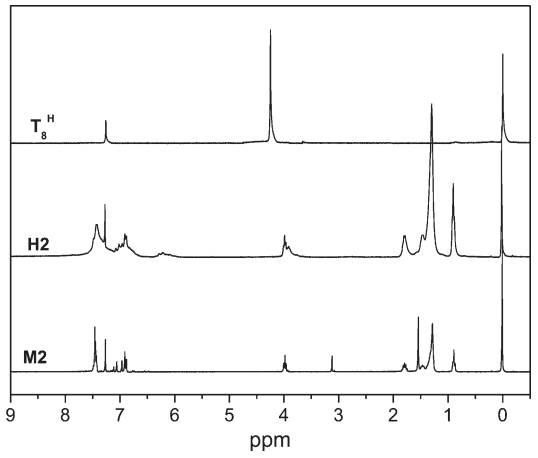

Figure 2. ^{1}H NMR spectra of $\mathbf{T_8^H}$, **M2**, and **H2**.

(feed ratio in 8:1) using Pt(dcp) as a catalyst, as shown in Scheme 1.

Solubilities and Film-Forming Properties. All the hybrids are readily soluble in various organic solvents such as chloroform, toluene, THF, and 1,2-dichloroethane. Solutions of the hybrids in THF (ca. 0.1 mg/mL) can be easily cast into films, whereas films of the monomers cannot be obtained under the same conditions, indicating incorporation of POSS endowed the resultant hybrids with good film formability.

Structural Characterization. Figure 1 shows the FTIR spectra of $\mathbf{T_8^H}$, **M2**, and **H2**. The absorption band of **M2** at 3289 cm^{-1} originating from the ≡C−H stretching vibration completely disappears in the spectrum of **H2**, and the strong characteristic absorption of Si−O−Si at 1110 cm^{-1} emerges in the spectrum of **H2**, suggesting that the POSS cage is incorporated into the NLO chromophores forming new hybrid **H2**. Similar results are also found in the spectra of **H1**, **H3**, and **H4**.

Figure 2 shows the ^{1}H NMR spectra of $\mathbf{T_8^H}$, **M2**, and **H2** in chloroform-*d*. The absorption of the acetylene proton in the ^{1}H NMR spectrum of **M2** which appears at 3.12 ppm as a singlet peak completely disappears in the ^{1}H NMR spectrum of the resulting hybrid **H2**. Meanwhile, new broad peaks at ca. 6.0−6.4 ppm are found, which are ascribed to olefin proton absorption of α- and *β*-adducts, indicating that the chromophores are covalently attached to the POSS core to form the molecular dispersed organic−inorganic hybrids.

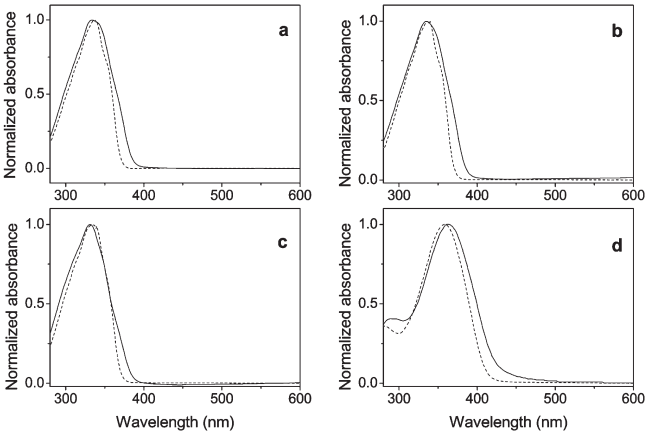

Figure 3. UV−vis absorption spectra of the hybrids (solid line) and corresponding monomers (dashed line) in THF solutions. (a) **M1** and **H1**; (b) **M2** and **H2**; (c) **M3** and **H3**; (d) **M4** and **H4**.

The ^{13}C NMR and ^{29}Si NMR spectra can be found in the Supporting Information (Figures S1 and S2). The signals at ca. 77 and 84 ppm corresponding to the acetylenic carbons in **M2** completely disappear in the ^{13}C NMR spectrum of **H2**, further proving the POSS cages are successfully introduced into stilbene chromophores. Simultaneously, the −O*C*H$_2$− group displays doublet peaks (67.6 and 67.5 ppm) in the ^{13}C NMR spectrum of **H2**, and the ^{29}Si NMR spectrum of **H2** shows new peaks at ca. −81.03 and −78.08 ppm, confirming the resulting hybrids are the mixture of α- and *β*-addition products. Integration of the ^{29}Si NMR signals yields the mixture ratios (α/*β* adducts) of 39/61, 43/57, 42/58, and 42/58 for **H1**−**H4**, respectively. In addition, on the basis of the integration of the ^{29}Si NMR signals, we also found that approximate seven chromophores in average were incorporated into one POSS molecule in the hybrids.

Linear Optical Properties. As can be seen from Figure 3a−d, the THF solutions of **H1**−**H4** show strong absorption peaks located at 336, 339, 335, and 360 nm, respectively, and display high transparency in the visible region. Simultaneously, it is also found that alkoxy chain length exerts little influence on the UV absorption spectra of **H1**−**H3** (the absorption profiles of **H1**−**H3** are similar). However, the absorption peak of **H4** is red-shifted, which may attribute to stronger intramolecular charge transfer (ICT) in the excited state.[40,41] Although the hybrids and their corresponding monomers show nearly the same λ_{max}, broader absorption bands are observed in the UV spectra of the hybrids, which may originate from the "$\sigma-\pi$ conjugation effect" of Si−C═C− in the hybrids.[42]

Thermal Analysis of the Hybrids. As shown in Figure 4, **H1**−**H4** offer the thermal decomposition temperatures (T_d, 5 mass % loss) at ca. 280, 320, 310, and 280 °C, which are 20−60 °C greater than their corresponding monomers, implying that the POSS core enhances the thermal stability of the hybrids.[8,43] The enhancement in thermal stability could attribute to two major reasons. First, the very uniform dispersion of silica nanoparticles within the hybrids provides significant added heat capacity, thereby limiting degradation. Second, as organic segment is decomposed away from the surface, the remaining residue becomes enriched in silica and provides a barrier to further heat attack.[38,44,45] Simultaneously, no crystallization peaks and glass transition temperature are detectable when the hybrids are heated to 250 °C in the DSC measurements. The amorphous character may result from the rigid Si−vinyl-linked moieties projecting off the spherical POSS core in three dimensions, thus minimizing intra

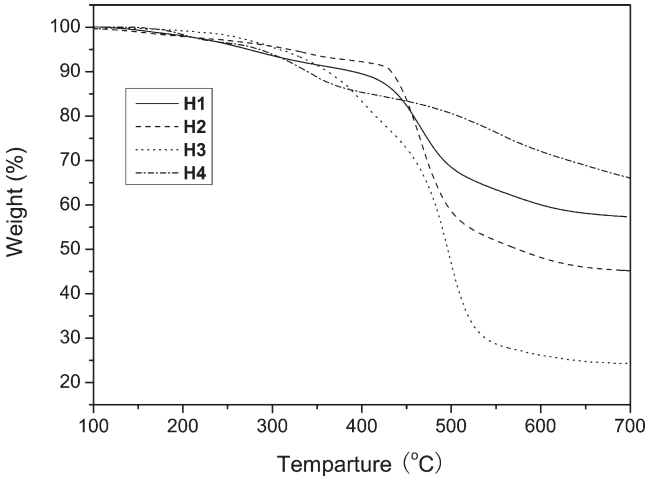

Figure 4. TGA thermograms of **H1**−**H4** at a ramp rate of 20 °C/min in nitrogen flow.

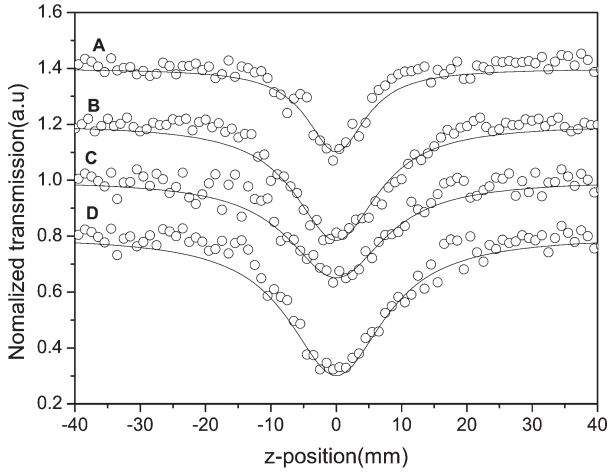

Figure 5. Normalized open-aperture *Z*-scan transmittance of (A) **H1**, (B) **H2**, (C) **H3**, and (D) **H4** in THF using 4 ns pulses at 532 nm. The curves have been vertically shifted for clarity. Solid lines represent theoretical fits.

or inter $\pi-\pi$ interactions.[46] This structure will effectively prevent intermolecular stacking resulting from joule heating during device operation.[43,47]

Nonlinear Absorption Properties. The nonlinear absorption behavior of **H1**−**H4** in THF was evaluated by the *Z*-scan technique under an open aperture configuration. As shown in Figure 5, the linear absorption spectra of **H1**−**H4** show nearly no linear absorption at 532 nm, which promises low intensity loss and little temperature change by photon absorption during the NLO measurements. In theory, the normalized transmittance for the open aperture configuration can be written as[35]

$$T(z, s = 1) = \sum_{m=0}^{\infty} \frac{[-q_0(z)]^m}{(m+1)^{3/2}}, \quad \text{for } |q_0| < 1 \qquad (1)$$

where $q_0(z) = \beta I_0(t) L_{\text{eff}}/(1 + z^2/{z_0}^2)$, β is the nonlinear absorption coefficient, $I_0(t)$ is the intensity of laser beam at focus ($z = 0$), $L_{\text{eff}} = [1 - \exp(-\alpha_0 L)]/\alpha_0$ is the effective thickness with α_0 the linear absorption coefficient, L is the sample thickness, z_0 is the diffraction length of the beam, and z is the sample position. The results from the *Z*-scan experiments are demonstrated in Figure 5. The solid lines in

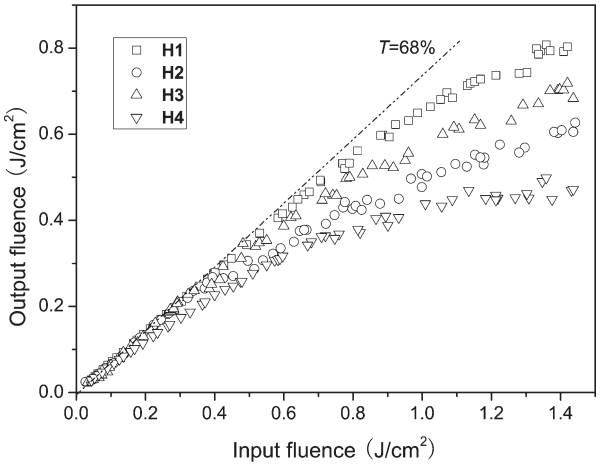

Figure 6. Optical limiting responses to 4 ns, 1 Hz pulses of 532 nm laser light in THF solutions of **H1**−**H4** with a linear transmittance of 68%.

Figure 5 are theoretical curves from eq 1. The data collected under the open-aperture configuration indicate that they all exhibit good nonlinear absorption properties with effective β values of 1.81×10^{-11} m W^{-1} (**H1**), 1.90×10^{-11} m W^{-1} (**H2**), 1.85×10^{-11} m W^{-1} (**H3**), and 2.56×10^{-11} m W^{-1} (**H4**). These β values are in the same order of magnitude as the β value for 4,4′-bis(di-*n*-butylamino)stilbene.[37] Under the same experimental conditions, the nonlinear absorption performance (β) of **M1**−**M4** are evaluated to be 1.64×10^{-11}, 1.71×10^{-11}, 1.68×10^{-11}, and 2.26×10^{-11} m W^{-1}, respectively. The enhanced effect of nonlinear absorption performance (β) in the hybrids may originate from the "$\sigma-\pi$ conjugation effect" of Si−C═C− in the hybrids. **H4** exhibits the strongest NLO absorption effect, which may be assigned to the larger π-electron delocalization of molecules and stronger intramolecular charge transfer (ICT) in the excited state.[40] This is consistent with the analysis of the linear absorption and emission spectra.

Optical Limiting Properties. As discussed in the previous sections, **H1**−**H4** possess obvious nonlinear absorption; therefore, an optical limiting of nanosecond laser pulses is expected from these hybrids. To demonstrate this, optical limiting measurements were conducted at 532 nm using 4 ns laser pulses. Figure 6 shows the optical limiting behaviors of **H1** (concentration $c = 1.85$ mg/mL), **H2** ($c = 2.16$ mg/mL), **H3** ($c = 2.60$ mg/mL), and **H4** ($c = 2.12$ mg/mL) at the same linear transmittance ($T = 68\%$) in THF. At very low incident fluence, the output fluence of the solutions increases linearly with the incident fluence obeying Beer's law. However, at high incident fluence, the transmittance of the solutions decreases with the increase of input fluence, and a nonlinear relationship is observed between the output and input fluence, with a further increase in the incident fluence; the output fluence of the solutions reaches a plateau, suggesting the occurrence of the optical limiting effect.

Experiments with THF solvent alone afforded no detectable OL effect, indicating that the solvent contribution is negligible. The limiting threshold (incident fluence at which the output fluence starts to deviate from linearity) and amplitude (maximum output fluence) are summarized in Table 1. Simultaneously, it is also found that the optical limiting characteristics of these hybrids are influenced by different substituents of stilbene chromophores. **H4** with a NO_2 group clearly exhibits the lowest limiting threshold (0.24 J/cm^2) and limiting amplitude (0.51 J/cm^2) among these four hybrids. Their optical limiting properties appears the trend of **H4** > **H2** > **H3** > **H1**. This is agreement with

Table 1. Optical Limiting and Nonlinear Absorption Properties of H1−H4

hybrid	limiting threshold[a] (J/cm^2)	limiting amplitude[b] (J/cm^2)	β[c] (m/W)
H1	0.40	0.78	1.81×10^{-11}
H2	0.35	0.61	1.90×10^{-11}
H3	0.38	0.69	1.85×10^{-11}
H4	0.24	0.51	2.56×10^{-11}

[a] Incident fluence at which the output fluence starts to deviate from linearity. [b] Maximum output fluence. [c] Measured by the *Z*-scan technique with an 4 ns Nd:YAG laser system at 1 Hz repetition rate and 532 nm wavelength.

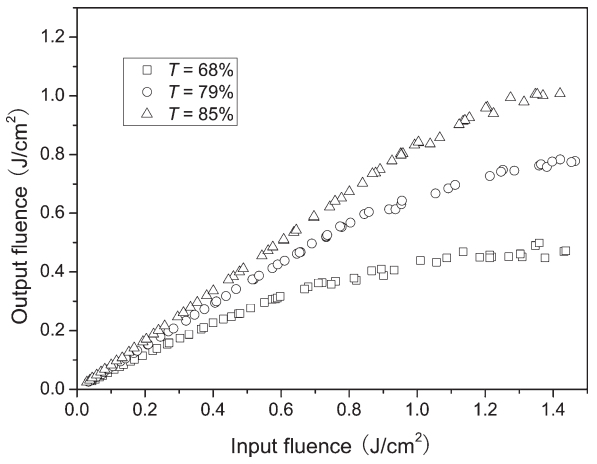

Figure 7. Optical limiting responses to 4 ns, 1 Hz pulses of 532 nm laser light in THF solutions of **H4** with different linear transmittances.

the nonlinear absorbance results obtained from *Z*-scan measurement. In addition, we measured the UV−vis absorption spectra of these hybrids before and after the laser irradiation and found that the pattern and intensity of UV−vis absorption spectra have almost no change, hinting that the hybrids possess good photostability.

Figure 7 shows the optical limiting performances of **H4** in THF at different concentrations. It can be found that higher concentration (lower transmittance) solution exhibits better performances. Similar results were also found by Kojima's[48] and our previous publications.[49] Solution with higher concentration has more molecules per unit volume, thereby absorbing the energy of the harsh laser more efficiently.

Reverse saturable absorption (RSA) or two-photon absorption (TPA) mechanism is often proposed for optical limiting of organic compounds. Generally, TPA occurs under the laser irradiation of picosecond or shorter pulses. RSA occurs under nanosecond or longer pulses, rather than a picosecond time scale, because of the different excited-state lifetimes involved in a multilevel energy process.[50] In this work, the hybrids are excited by the laser with 4 ns pulse width at 532 nm. Therefore, we consider that RSA could be major mechanism for the optical limiting of these hybrids.

The optical limiting property of RSA molecules can be also evaluated by the ratio of the excited-state absorption cross section (σ_{ex}) to the ground-state absorption cross section (σ_0) of molecules, which was defined as $\sigma_{ex}/\sigma_0 = \ln T_{sat}/\ln T_0$. T_{sat} is the saturated transmittance for high degrees of excitation.[51] The larger the value of σ_{ex}/σ_0 is, the better the optical limiting performance is. In our experimental setup, although we are unable to reach the saturable transmittance for these compounds, we can use the transmittance at 1.42 J/cm^2 to calculate the lowest bound for σ_{ex}/σ_0. On the basis of the experiment data illustrated in Figure 6, the calculated values of σ_{ex}/σ_0 for **H1**−**H4** are 1.5, 1.8, 2.2, and 2.8, respectively, further confirming that their optical limiting mechanisms are mainly originated from reverse saturable absorption resulting from the large excited-state absorption cross section.

Conclusions

In conclusion, four starlike stilbene-containing silsesquioxanes organic−inorganic hybrid materials were successfully synthesized and characterized. It is found that the combination of inorganic POSS core with stilbene NLO chromophores endows the resulting hybrids with novel optical limiting properties, good film formability, and enhanced thermal stability. In addition, it is also found that nitro-substituted **H4** exhibits better performances than alkoxy-substituted hybrids (**H1**, **H2**, and **H3**), which may be attributed to the larger π-electron delocalization and charge transfer ability of the nitro group than that of the alkoxy group. The work provides a novel path for designing new optical materials with high thermal stability and good optical limiting property.

Acknowledgment. This research was financially supported by the National Natural Science Fund of China (Grants 20974018 and 20971021), Ph.D. Program Foundation of Ministry of Education of China (No. 20070255012), Shanghai Leading Academic Discipline Project (No. B603) and Open Project of the State Key Laboratory of Crystal Materials (KF0809), the Program of Introducing Talents of Discipline to Universities (No. 111-2-04), and China Postdoctoral Science Foundation (20080440563 and 200902193).

Supporting Information Available: Tables with NMR data, ^{13}C NMR spectra of **M2** and **H2**, and ^{29}Si NMR spectra of $\mathbf{T_8^H}$ and **H2**. This material is available free of charge via the Internet at http://pubs.acs.org.

References and Notes

(1) Yin, S.; Xu, H.; Su, X.; Li, G.; Song, Y.; Lam, J. W. Y.; Tang, B. Z. *J. Polym. Sci., Part A: Polym. Chem.* **2006**, *44*, 2346–2357.
(2) Su, X.; Xu, H.; Yang, J.; Lin, N.; Song, Y. *Polymer* **2008**, *49*, 3722–3730.
(3) Su, X.; Xu, H.; Guo, Q.; Shi, G.; Yang, J.; Song, Y.; Liu, X. *J. Polym. Sci., Part A: Polym. Chem.* **2008**, *46*, 4529–4541.
(4) Wang, X.; Wu, J.; Xu, H.; Wang, P.; Tang, B. Z. *J. Polym. Sci., Part A: Polym. Chem.* **2008**, *46*, 2072–2083.
(5) Wang, X.; Guang, S.; Xu, H.; Su, X.; Yang, J.; Song, Y.; Lin, N.; Liu, X. *J. Mater. Chem.* **2008**, *18*, 4202–4209.
(6) Molnar, R. M.; Bodnar, M.; Hartmann, J. F.; Borbely, J. *Colloid Polym. Sci.* **2009**, *287*, 739–744.
(7) Su, X.; Guang, S.; Xu, H.; Liu, X.; Li, S.; Wang, X.; Deng, Y.; Wang, P. *Macromolecules* **2009**, *42*, 8969–8976.
(8) Xu, H.; Yang, B.; Wang, J.; Guang, S.; Li, C. *Macromolecules* **2005**, *38*, 10455–10460.
(9) Xu, H.; Kuo, S.-W.; Lee, J.-S.; Chang, F.-C. *Macromolecules* **2002**, *35*, 8788–8793.
(10) Tamaki, R.; Choi, J.; Laine, R. M. *Chem. Mater.* **2003**, *15*, 793–797.
(11) Choi, J.; Yee, A. F.; Laine, R. M. *Macromolecules* **2004**, *37*, 3267–3276.
(12) Haddad, T. S.; Lichtenhan, J. D. *Macromolecules* **1996**, *29*, 7302–7304.
(13) Pyun, J.; Matyjaszewski, K. *Macromolecules* **2000**, *33*, 217.
(14) Mather, P. T.; Jeon, H. G.; Romo-Uribe, A.; Haddad, T. S.; Lichtenhan, J. D. *Macromolecules* **1999**, *32*, 1194–1203.
(15) Zheng, L.; Farris, R. J.; Coughlin, E. B. *Macromolecules* **2001**, *34*, 8034–8039.
(16) Lee, A.; Lichtenhan, J. D. *Macromolecules* **1998**, *31*, 4970.
(17) Xu, H.; Yang, B.; Wang, J.; Guang, S.; Li, C. *J. Polym. Sci., Part A: Polym. Chem.* **2007**, *45*, 5308–5317.
(18) Markovic, E.; Ginic-Markovic, M.; Clarke, S.; Matisons, J.; Hussain, M.; Simon, G. P. *Macromolecules* **2007**, *40*, 2694–2701.

(19) Bolln, C.; Tsuchida, A.; Frey, H.; Mülhaupt, R. *Chem. Mater.* **1997**, 9.
(20) Yang, B.; Xu, H.; Yang, Z.; Liu, X. *J. Mater. Chem.* **2009**, *19*, 9038–9044.
(21) Su, H. W.; Chen, W. C. *Mater. Chem. Phys.* **2009**, *114*, 736–741.
(22) Liu, Y. L.; Fangchiang, M. H. *J. Mater. Chem.* **2009**, *19*, 3643–3647.
(23) Chen, K.-B.; Chang, Y.-P.; Yang, S.-H.; Hsu, C.-S. *Thin Solid Films* **2006**, *514*, 103–109.
(24) Lo, M. Y.; Zhen, C.; Lauters, M.; Jabbour, G. E.; Sellinger, A. *J. Am. Chem. Soc.* **2007**, *129*, 5808–5809.
(25) Xiao, Y.; Liu, L.; He, C.; Chin, W. S.; Lin, T.; Mya, K. Y.; Huang, J.; Lu, X. *J. Mater. Chem.* **2006**, *16*, 829–836.
(26) Imae, I.; Kawakami, Y. *J. Mater. Chem.* **2005**, *15*, 4581–4583.
(27) Lo, M. Y.; Ueno, K.; Tanabe, H.; Sellinger, A. *Chem. Rec.* **2006**, *6*, 157–168.
(28) Miyake, J.; Chujo, Y. *Macromol. Rapid Commun.* **2008**, *29*, 86–92.
(29) Soh, M. S.; Yap, A. U. J.; Sellinger, A. *Eur. Polym. J.* **2007**, *43*, 315–327.
(30) Moon, J. H.; Seo, J. S.; Xub, Y.; Yang, S. *J. Mater. Chem.* **2009**, *19*, 4687–4691.
(31) Ceyhan, T.; Yüksek, M.; Yağlíoğlu, H. G.; Salih, B.; Erbil, M. K.; Elmalí, A.; Bekaroğlu, Ö. *Dalton Trans.* **2008**, 2407–2413.
(32) Su, X.; Xu, H.; Deng, Y.; Li, J.; Zhang, W.; Wang, P. *Mater. Lett.* **2008**, *62*, 3818–3820.
(33) Agaskar, P. A. *J. Am. Chem. Soc.* **1989**, *111*, 6858–6859.
(34) Apfel, M. A.; Finkelmann, H.; Janini, G. M.; Laub, R. J.; Luehmann, B. H.; Price, A.; Roberts, W. L.; Shaw, T. J.; Smith, C. A. *Anal. Chem.* **1985**, *57*, 651–658.
(35) Sheik-Bahae, M.; Said, A. A.; Wei, T.-H.; Hagan, D. J.; Stryland, E. W. V. *IEEE J. Quantum Electron.* **1990**, *26*, 760–769.
(36) Qu, S.; Song, Y.; Du, C.; Wang, Y.; Gao, Y.; Liu, S.; Li, Y.; Zhu, D. *Opt. Commun.* **2001**, *196*, 317–323.
(37) Ehrlich, J. E.; Wu, X. L.; Lee, I.-Y. S.; Hu, Z.-Y.; Röckel, H.; Marder, S. R.; Perry, J. W. *Opt. Lett.* **1997**, *22*, 1843–1845.
(38) Sulaiman, S.; Bhaskar, A.; Zhang, J.; Guda, R.; Goodson, T., III.; Laine, R. M. *Chem. Mater.* **2008**, *20*, 5563–5573.
(39) Zhang, C.; Babonneau, F.; Bonhomme, C.; Laine, R. M.; Soles, C. L.; Hristov, H. A.; Yee, A. F. *J. Am. Chem. Soc.* **1998**, *120*, 8380–8391.
(40) Bhaskar, A.; Ramakrishna, G.; Lu, Z.; Twieg, R.; Hales, J. M.; Hagan, D. J.; VanStryland, E.; Goodson, T. *J. Am. Chem. Soc.* **2006**, *128*, 11840–11849.
(41) Ronchi, M.; Pizzotti, M.; Biroli, A. O.; Righetto, S.; Ugo, R.; Mussini, P.; Cavazzini, M.; Lucenti, E.; Salsa, M.; Fantucci, P. *J. Phys. Chem. C* **2009**, *113*, 2745–2760.
(42) Chen, Z.-K.; Huang, W. *Macromolecules* **2000**, *33*, 9015–9025.
(43) Markovic, E.; Matisons, J.; Hussain, M.; Simon, G. P. *Macromolecules* **2007**, *40*, 4530–4534.
(44) Asuncion, M. Z.; Laine, R. M. *Macromolecules* **2007**, *40*, 555–562.
(45) Markovic, E.; Ginic-Markovic, M.; Clarke, S.; Matisons, J.; Hussain, M.; Simon, G. P. *Macromolecules* **2007**, *40*, 2694–2701.
(46) Yoonlo, M.; Ueno, K.; Tanabe, H.; Sellinger, A. *Chem. Rec.* **2006**, *6*, 157–168.
(47) Fina, A.; Abbenhuis, H. C. L.; Tabuani, D.; Frache, A.; Camino, G. *Polym. Degrad. Stab.* **2006**, *91*, 1064–1070.
(48) Kojima, Y.; MatsuHoka, T.; Sato, N.; Takahashi, H. *Macromolecules* **1995**, *28*, 2893–2896.
(49) Su, X.; Wu, L.; Yin, S.; Xu, H.; Wu, Z.; Song, Y.; Tang, B. Z. *J. Macromol. Sci., Pure Appl. Chem.* **2007**, *44*, 691–697.
(50) Sun, W. F.; Bader, M. M.; Carvalho, T. *Opt. Commun.* **2003**, *215*, 185–190.
(51) Perry, J. W.; Mansour, K.; Marder, S. R.; Perry, K. J.; Daniel Alvarez, J.; Choong, I. *Opt. Lett.* **1994**, *19*, 625–627.